

A Computational Study of the Proton-Transfer Chemistry of the Silaformyl Anion

Jon A. Rusho,[†] Mark S. Gordon,^{*,†} Niels H. Damrauer,[‡] and Robert Damrauer^{*,‡}

Contribution from the Chemistry Department, Iowa State University, Ames, Iowa 50011-3111, and Chemistry Department, University of Colorado at Denver, Denver, Colorado 80217-3364

Received July 3, 1997. Revised Manuscript Received January 2, 1998

Abstract: Proton-transfer reactions involving the silaformyl anion, HSiO^- , and its conjugate acids, HSiOH and H_2SiO , have been investigated with ab initio methods. Calculations through fourth-order perturbation theory suggest possible routes for proton transfer. Accurate estimates for the acidity of H_2SiO and HSiOH are presented and discussed in light of earlier experimental estimates.

Introduction

The gas-phase ion chemistry of $[\text{H}_2\text{SiO}]^-$,¹ which is prepared by collision-induced dissociation of H_3SiO^- in a tandem flowing afterglow selected ion flow tube (FA-SIFT), has been studied in detail.² Both experimental and computational studies suggest strongly² that the structure of $[\text{H}_2\text{SiO}]^-$ is that of the silaformyl anion, HSiO^- . Mechanistic considerations of the reactions of $[\text{H}_2\text{SiO}]^-$ and neutrals such as CO_2 , CS_2 , COS , SO_2 , and O_2 have established the structural identity of the anion.² Related detailed computational studies³ carried out on the $\text{CO}_2 + \text{HSiO}^-$ potential energy surface at the MP4/6-311++G(d,p)/MP2/6-31++G(d,p) level are largely consistent with the earlier mechanistic proposals.²

Some of the reactions studied earlier, particularly those with reference acids that typically are used to establish the proton affinities of anions, raise certain questions that are not amenable to experimental study.² Not only was the acidity of the parent acid of HSiO^- not accurately determined ($\Delta G_{\text{acid}}^\circ = 356 \pm 8$ kcal/mol) because of a minor contamination of H_3SiO^- and side reactions with reference acids, but the identity of the corresponding acid was unknown, although both HSiOH and H_2SiO were suggested as reasonable possibilities based on experimental and computational work carried out on the neutral species with the composition $[\text{H}_2\text{SiO}]$.^{4–10} Thus, the three structures of lowest energy are cis HSiOH , trans HSiOH , and H_2SiO , all having energies computed to be within about 3 kcal/mol. Barriers to cis–trans interconversion have been computed to be fairly low (~ 8 kcal/mol),^{7,8,10} although the conversion of HSiOH to H_2SiO surmounts a large barrier (~ 60 kcal/mol).^{7,8}

In the current work, we examine the pathways for proton abstraction by HSiO^- from HSiOH and H_2SiO to probe questions about the identity of the parent acid. In addition, acidity computations for HSiOH and H_2SiO are reported. High-level ab initio methods with significant electron correlation are required to obtain reliable results.

Computational Methods

The reactions were initially probed by using the restricted Hartree–Fock (RHF) method with the 6-31++G(d,p) basis set.^{11–15} This basis set has diffuse and polarization functions to describe the anions and anion–molecule complexes reasonably well. The structures were determined by optimizing the geometry with use of analytical gradient methods. To better describe the potential energy surfaces, we refined the RHF structures using Møller–Plesset second-order perturbation theory (MP2)¹⁶ with the same basis set (6-31++G(d,p)).

The identification of stationary points as minima or saddle points was determined by calculation and diagonalization of the Hessian force constant matrix (matrix of energy second derivatives). Transition states were determined at both the RHF and MP2 levels of theory with the 6-31++G(d,p) basis set.

Once the transition states were located, minimum energy reaction paths connecting reactants with products, the so-called intrinsic reaction paths (IRP), were calculated by using the Gonzalez–Schlegel second-order method^{17,18} normally with a step size of $0.3 \text{ amu}^{1/2} \cdot \text{bohr}$; steps as small as $0.01 \text{ amu}^{1/2} \cdot \text{bohr}$ were used in regions close to minima. IRP calculations were carried out at both the RHF and MP2 levels of theory with the 6-31++G(d,p) basis set.

Once the structures of the stationary points were determined at the MP2/6-31++G(d,p) level of theory, more advanced levels of theory were employed to obtain more reliable energetics. The levels of theory used for final energetics were fourth-order perturbation theory (MP4) and coupled-cluster with single and double excitations and triple excitations estimated perturbatively (CCSD(T)).¹⁹ The MP4 calcula-

[†] Iowa State University.

[‡] University of Colorado at Denver.

(1) This notation is used to signify the composition but not the structure of ions.

(2) Gronert, S.; O'Hair, R. A. J.; Prodnuk, S.; Sülzle, D.; Damrauer, R.; DePuy, C. H. *J. Am. Chem. Soc.* **1990**, *112*, 997–1003.

(3) Shimizu, H.; Gordon, M. S.; Damrauer, R.; O'Hair, R. A. J. *Organometallics* **1995**, *14*, 2664–2671.

(4) Srinivas, R.; Böhme, D. K.; Sülzle, D.; Schwarz, H. *J. Phys. Chem.* **1991**, *95*, 9836–41.

(5) Kudo, T.; Nagase, S. *J. Organomet. Chem.* **1983**, *253*, C23–C26.

(6) Kudo, T.; Nagase, S. *J. Am. Chem. Soc.* **1985**, *107*, 2589–2595.

(7) Kudo, T.; Nagase, S. *Organometallics* **1986**, *5*, 1207–1215.

(8) Kudo, T.; Nagase, S. *J. Phys. Chem.* **1984**, *88*, 2833–2840.

(9) Gordon, M. S.; Pederson, L. A. *J. Phys. Chem.* **1990**, *94*, 5527–30.

(10) Ma, B.; Schaefer, H. F., III *J. Chem. Phys.* **1994**, *101*, 2734–39.

(11) Francl, M. M.; Pietro, W. J.; Hehre, W. J.; Binkley, J. S.; Gordon, M. S.; DeFree, D. J.; Pople, J. A. *J. Chem. Phys.* **1982**, *77*, 3654–3665.

(12) Krishnan, R.; Binkley, J. S.; Seeger, R.; Pople, J. A. *J. Chem. Phys.* **1980**, *72*, 650–654.

(13) McLean, A. D.; Chandler, G. S. *J. Chem. Phys.* **1980**, *72*, 5639–5648.

(14) Clark, T.; Chandrasekhar, J.; Spitznagel, G. W.; Schleyer, P. v. R. *J. Comput. Chem.* **1983**, *4*, 294–301.

(15) Frisch, M. J.; Pople, J. A.; Binkley, J. S. *J. Chem. Phys.* **1984**, *80*, 3265–3269.

(16) Møller, C.; Plesset, M. S. *Phys. Rev.* **1934**, *46*, 618–622.

(17) Gonzalez, C.; Schlegel, H. B. *J. Chem. Phys.* **1989**, *90*, 2154.

(18) Gonzalez, C.; Schlegel, H. B. *J. Phys. Chem.* **1990**, *94*, 5523–5527.

Table 1. MP2/6-31++G(d,p), MP4/6-311++G(d,p), and CCSD(T)/6-311++G(2df,2pd) Relative Energies (in kcal/mol) of the Reactants^a

reactants	MP2//MP2	MP4//MP2	CCSD(T)//MP2	ZPE
HSiO ⁻	0.0	0.0	0.0	5
HOSi ⁻	+39.1	+39.1	+35.8	8
<i>trans</i> -HSiOH	0.0	0.0	0.0	14
<i>cis</i> -HSiOH	0.5	0.5	0.3	13
H ₂ SiO	-1.0	0.2	+2.6	12

^a ZPE is the MP2/6-31++G(d,p) harmonic zero-point energy.

tions were carried out by using the 6-311++G(d,p) basis,^{11–15} and the CCSD(T) calculations were performed with the 6-311++G(2df,2pd) basis set.^{11–15} The notation A/B indicates that an energy is calculated by method A with a geometry optimized by method B.

Localized molecular orbital (LMO) calculations²⁰ were carried out on select minima and transition states to examine the nature of the bonding as well as how the anion and neutral species interact to form stationary points on the potential energy surfaces.

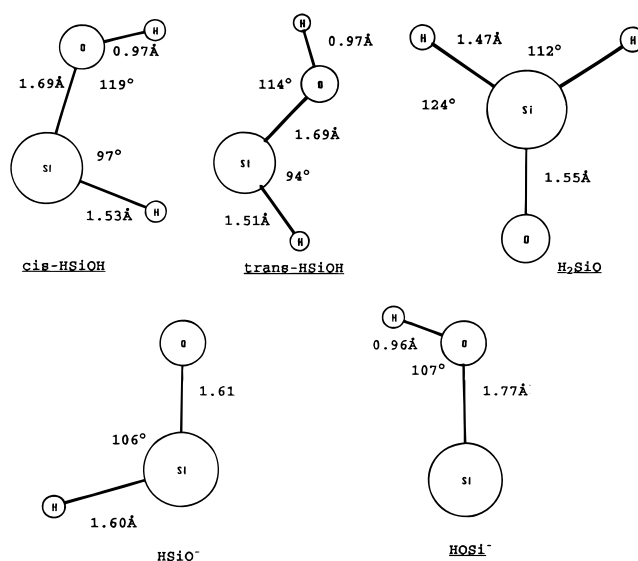
Ion–molecule complexes were located by positioning neutral species 3–5 Å away from an anion and allowing full geometry optimization. Variations in orientation of the ion with respect to the neutral substrate resulted in different complexes from the same reactants. Minima, as well as first- and second-order saddle points, were located with this technique. The second-order saddle points were used to locate minima or first-order saddle points by following the IRP's associated with the imaginary frequencies.

Reaction energies in the following discussions are reported relative to the energy of HSiO⁻ + *trans*-HSiOH, the lowest-energy anion/neutral combination prior to zero-point energy correction.

Calculations were carried out with either GAMESS²¹ or Gaussian 92/DFT,²² with their respective built-in basis sets.

Results and Discussion

1. Reactants. The relative energies of HSiO⁻, HOSi⁻, HSiOH (*cis* and *trans*), and H₂SiO are presented at the MP2/6-31++G(d,p)//MP2/6-31++G(d,p), MP4/6-311++G(d,p)//MP2/6-31++G(d,p), and CCSD(T)/6-311++G(2df,2pd)//MP2/6-31++G(d,p) levels in Table 1.²³ Figure 1 shows the geometries of these species optimized at the MP2/6-31++G(d,p) level of theory. To the extent that comparisons can be made, these data are consistent with previous computations with HSiO⁻ being considerably lower in energy than HOSi⁻, and the neutrals and *cis* and *trans* HSiOH and H₂SiO having very similar energies.^{2,7,9,10} HSiOH has stable *cis* and *trans* isomers with a dihedral angle of 97.6° at the transition state between them. The CCSD(T)/6-311++G(2df,2pd) *cis*-to-*trans* barrier height is 9 kcal/mol (Table 2, including zero-point energy corrections calculated at the MP2/6-31++G(d,p) level of theory). In this transition state the H–O and O–Si distances have contracted by 0.02 and 0.03 Å relative to the *cis* structure. On both the RHF and MP2 surfaces, H₂SiO is structurally similar to formaldehyde. At the CCSD(T)/6-311++G(2df,2pd)//MP2/6-31++G(d,p) level of theory, which is the highest

**Figure 1.** Neutral and ionic reactant geometries at the MP2/6-31++G(d,p) level of theory. H₂SiO has C_{2v} symmetry; the remaining species have C_s symmetry.**Table 2.** MP2/6-31++G(d,p), MP4/6-311++G(d,p), and CCSD(T)/6-311++G(2df,2pd) Barrier (in kcal/mol) to Conversion from *cis*- to *trans*-HSiOH, Relative to *cis*-HSiOH and *trans*-HSiOH^a

	MP2	MP4	CCSD(T)
<i>cis</i> -HSiOH	+9	+9	+9
<i>trans</i> -HSiOH	+7	+7	+7

^a Zero-point correction at 298.15 K is included.

computational level used to date, it is slightly less stable than *cis* or *trans* HSiOH (Table 1).²³

HSiO⁻ and HOSi⁻ can be compared with the HSiO and HOSi radicals that Schaefer and co-workers recently have examined using configuration interaction (CISD) calculations with a triple- ζ plus double polarization (TZ2P) basis set with and without higher angular momentum functions and diffuse functions [TZ2P(f,d) and TZ2P(f,d)+diff].²⁴ All four species have similar bent geometries, although the anions have longer bond lengths as would be expected with an extra electron in the system. The silicon–oxygen separation is 1.64 Å in the HOSi radical at the CISD/TZ2P(f,d)+diff level of theory versus 1.77 Å for HOSi⁻ at the MP2/6-31++G(d,p) level. The HSiO radical, on the other hand, has an Si–O distance of 1.51 Å, while the Si–O bond distance in HSiO⁻ is 1.61 Å. Although rigorous comparisons between different levels of theory cannot be made, it is clear for both the radicals and the anions that a significant Si–O bond shortening occurs between the HOSi and HSiO species. The Si–O bond lengths of the HOSi radical and the HOSi⁻ and HSiO⁻ anions are all in the range expected for single Si–O bonds, while that for HSiO is clearly in the range of the Si–O double bond (compare the bond in H₂SiO of 1.51–1.55 Å).²⁵ These conclusions are further supported by localized orbital calculations²⁰ that give the Lewis structures shown in Figure 2 for these radicals and anions. These data demonstrate clearly that only HSiO has a Si–O double bond. The discrepancy in relative energetics (HOSi < HSiO vs HOSi⁻ > HSiO⁻) can be attributed to two factors: (1) The HSiO radical is apparently higher in energy than HOSi due to a tradeoff between the weak π bond between oxygen and silicon and a

(19) Noga, J.; Bartlett, R. J. *J. Chem. Phys.* **1987**, *86*, 7041–7050.(20) Edmiston, C.; Ruedenberg, K. *Rev. Mod. Phys.* **1963**, *35*, 457–465.(21) Schmidt, M. W.; Baldridge, K. K.; Boatz, J. A.; Jensen, J.; Koseki, S.; Gordon, M. S.; Nguyen, K. A.; Windus, T. L.; Elbert, S. T. *QCPE Bull.* **1990**, *10*, 52–54.

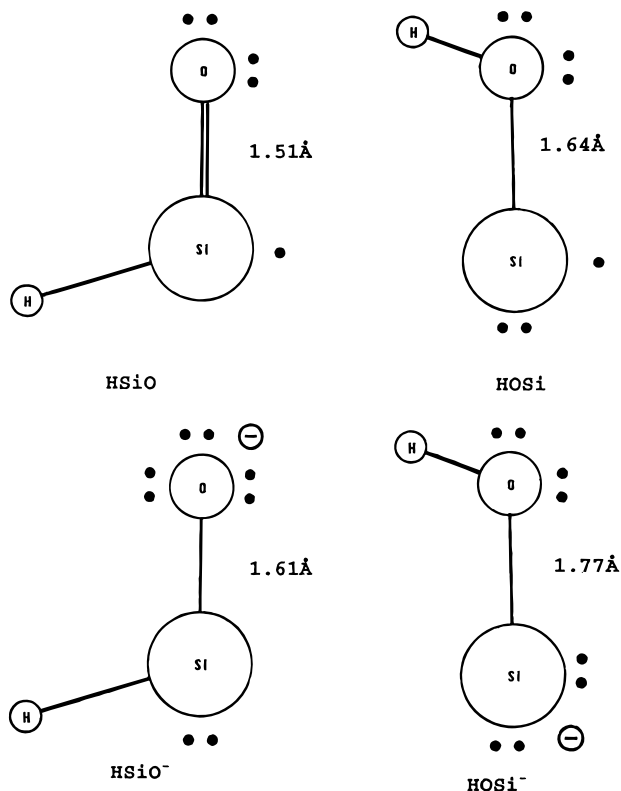
(22) Gaussian 92/DFT, R. G. 3.; Frisch, M. J.; Trucks, G. W.; Schlegel, H. B.; Gill, P. M. W.; Johnson, B. G.; Wong, M. W.; Foresman, J. B.; Robb, M. A.; Head-Gordon, M.; Replogle, E. S.; Gomperts, R.; Andres, J. L.; Raghavachari, K.; Binkley, J. S.; Gonzalez, C.; Martin, R. L.; Fox, D. J.; Defrees, D. J.; Baker, J.; Stewart, J. J. P.; Pople, J. A. Gaussian, Inc.: Pittsburgh, PA, 1993.

(23) The absolute energies are supplied in Supporting Information. See the current masthead for ordering instructions.

(24) Yamaguchi, Y.; Xie, Y.; Kim, S.; Schaefer, H. F., III. *J. Chem. Phys.* **1996**, *105*, 1951–1958.

Table 3. ΔH_{acid} (in kcal/mol) for Neutral Species at 298.15 K

reaction	MP2//MP2	MP4//MP2	CCSD(T)//MP2
<i>cis</i> -HSiOH \rightarrow HOSi ⁻ + H ⁺	389	392	390
<i>trans</i> -HSiOH \rightarrow HOSi ⁻ + H ⁺	389	391	389
<i>trans</i> -HSiOH \rightarrow HSiO ⁻ + H ⁺	347	349	351
<i>cis</i> -HSiOH \rightarrow HSiO ⁻ + H ⁺	347	350	351
H ₂ SiO \rightarrow HSiO ⁻ + H ⁺	359	351	350

**Figure 2.** Lewis structures of anions and radicals.

weak Si-H bond in HSio versus a strong OH bond in HOSi. (2) Addition of an electron to the electropositive silicon atom in HOSi is energetically less favorable than addition of an electron to the very electronegative oxygen in HSio to produce HSiO⁻.

2. Gas-Phase Acidities. The gas-phase acidity is defined as the free energy difference ($\Delta G_{\text{acid}}^{\circ}$) for the reaction $\text{HA} \rightarrow \text{H}^+ + \text{A}^-$ at 298.15 K. In the experimental study² of HSiO⁻, a crude estimate of the acidity of its corresponding acid was reported ($\Delta G_{\text{acid}}^{\circ} = 356 \pm 8$ kcal/mol). As previously indicated, the identity of the conjugate acid cannot be directly determined in FA-SIFT gas-phase experiments, although H₂SiO or HSiOH are likely possibilities. Computations of acidities generally require extended basis sets and at least fourth-order perturbation theory to obtain reliable acidities.²⁶ Such calculations on H₂SiO and HSiOH (Table 3) suggest that the estimated error limits for the experimental determination of the acidity of the conjugate acid of HSiO⁻ probably are too small. Thus, at the CCSD(T)/6-311++G(2df,2pd)//MP2/6-31++G(d,p) level H₂SiO has a $\Delta G_{\text{acid}}^{\circ}$ of 343 kcal/mol.^{27,28} Both *cis* and *trans*

Table 4. MP2/6-31++G(d,p), MP4/6-311++G(d,p), and CCSD(T)/6-311++G(2df,2pd) Relative Energies (in kcal/mol), with Respect to HSiO⁻ + *trans*-HSiOH, of Combined Reactants^a

reactants	MP2//MP2	MP4//MP2	CCSD(T)//MP2
HSiO ⁻ + <i>c</i> -HSiOH	-1	-1	-1
HSiO ⁻ + <i>t</i> -HSiOH	0	0	0
HSiO ⁻ + H ₂ SiO	-3	-2	+1

^a *cis*- and *trans*-HSiOH are denoted as *c*-HSiOH and *t*-HSiOH, respectively. Energies are calculated by using the MP2 geometries and include harmonic zero-point energy corrections (at 298.15 K) relative to HSiO⁻ + *trans*-HSiOH calculated at the MP2/6-31++G(d,p) level of theory.

Table 5. MP2/6-31++G(d,p) and MP4/6-311++G(d,p) Energies (kcal/mol) Relative to HSiO⁻ + *trans*-HSiOH, Including MP2 Zero-Point Energy Corrections

no.	MP2	MP4	no.	MP2	MP4
1	-45	-42	TS1-1	-30	-28
2	-53	-48	TS2-3	-23	-15
3	-92	-83	TS4-5	-14	-12
4	-17	-16	TS6-6	-44	-40
5	-54	-49	TS3-3	-38	-30
6	-53	-49	TS7-8	-38	-35
7	-43	-40			
8	-56	-54			

Table 6. CCSD(T)/6-311++G(2df,2pd) Energies (in hartrees) of Selected Low-Energy Structures^a

no.	reactants	rel energy
1	HSiO ⁻ + HSiOH	-46
4	HSiO ⁻ + H ₂ SiO	-95
6	HSiO ⁻ + H ₂ SiO	-51

^a Relative energy (in kcal/mol) is relative to HSiO⁻ + HSiOH and includes MP2 zero-point energy corrections.

HSiOH have Si-H acidities near 383 kcal/mol but O-H acidities similar to that of H₂SiO near 344 kcal/mol. The values near 344 kcal/mol most closely correspond to the experimental value of 356 ± 8 kcal/mol. The discrepancy between the computational and experimental estimates, while small, suggests that the error limits placed on the experimental work may have been too narrow.² Because these acidity results do not lead to a clear choice of the identity of the parent acid of HSiO⁻, an examination of the potential energy surfaces of various proton-transfer reactions has been undertaken to attempt to elucidate the identity of the parent acid.

3. Proton-Transfer Reactions. (a) Overview. Gronert has recently examined the potential energy surfaces of a series of proton-transfer identity reactions, $\text{AH}_n + \text{A}^-\text{H}_{n-1} \rightarrow \text{AH}_{n-1} + \text{A}^-\text{H}_n$, of second and third row elements (CH₄, NH₃, H₂O, HF, SiH₄, PH₃, H₂S, and HCl) at several computational levels including G2+.²⁹ These reactions are shown to be dramatically different depending on the nature of A. The barrier to proton transfer for second and third row elements decreases as the electronegativity of A increases. Thus, the double well potential surface of $[\text{CH}_3\cdots\text{H}\cdots\text{CH}_3]^-$ with a significant barrier "monotonically" gives way to a single well potential with a stable,

(25) Corey, J. Y. In *The Chemistry of Functional Groups*; Patai, S., Rappaport, Z., Eds.; John Wiley and Sons: New York, 1989; pp 1-56.

(26) Gordon, M. S.; Davis, L. P.; Burggraf, L. W.; Damrauer, R. *J. Am. Chem. Soc.* **1986**, *108*, 7889-93.

(27) A standard ΔS estimate of 7 kcal/mol was used to interconvert $\Delta H_{\text{acid}}^{\circ}$ and $\Delta G_{\text{acid}}^{\circ}$. See ref 28 for further details.

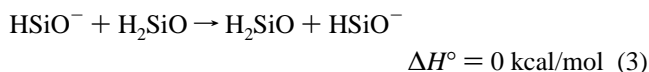
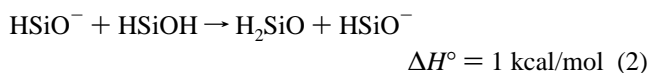
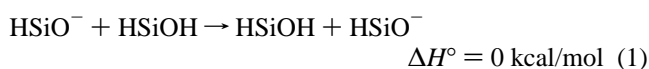
(28) Bartmess, J. E.; McIver, R. T. J. In *Gas-Phase Ion Chemistry*; Bowers, M. T., Ed.; Academic Press: New York, 1979; Vol. 2, pp 87-121.

(29) Gronert, S. *J. Am. Chem. Soc.* **1993**, *115*, 10258-10266.

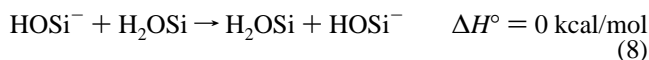
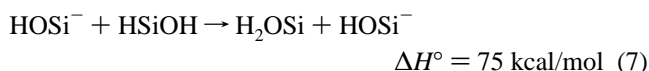
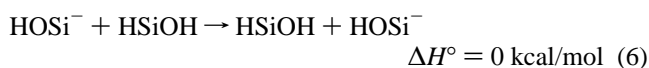
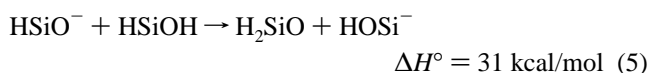
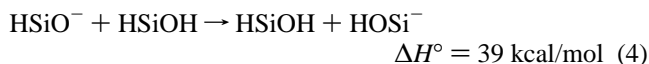
symmetric intermediate for $[F\cdots H\cdots F]^-$. It also was shown that third row elements experience higher barriers to proton transfer when compared with second row analogues of similar acidity.

In light of these studies, we now consider various proton-transfer reaction paths of HSiO^- with H_2SiO and HSiOH . Table 4²³ lists the relative energies of the possible anion and neutral combinations at the different levels of theory. Table 5 provides the relative energies for all the complexes and transition states to be discussed at the MP2 and MP4 levels of theory. Table 6 lists the energies of selected low-energy complexes at the CCSD(T) level of theory. A general examination of the reaction coordinates leading to these selected complexes (see Figures 3–7 below) suggests that it is energetically possible for these reactions to proceed via one or more intermediate ion–molecule complexes because the initial exothermicity due to complex formation is larger than the barriers to subsequent intramolecular rearrangement and dissociation to products. Such general results are reminiscent of earlier computational studies of silicon ion–molecule reactions,^{3,30} in which ion–molecule complexes lower in energy (10–50 kcal/mol) than the separated reactants form and subsequently undergo further conversion through a transition state whose energy is below the reactant (entrance channel) energy. The effect of transition state barrier heights on the reaction rates of ion–molecule reactions, particularly when the barrier height is lower in energy than the entrance channel energy, has been the subject of considerable study.^{31,32}

(b) Intermolecular Proton-Transfer Reactions. Three reactions between the base, HSiO^- , and acids, HSiOH and H_2SiO , have been examined in searching their proton-transfer potential energy surfaces (eqs 1–3). A number of other proton



transfer reactions involving HOSi^- have been examined as well (eqs 4–8), but these are considered to be chemically unrealistic



in trying to identify the parent acid because of the much higher energy of HOSi^- relative to HSiO^- . The ΔH° values (in kcal/mol) computed at the CCSD(T)/6-311++G(2df,2pd) level

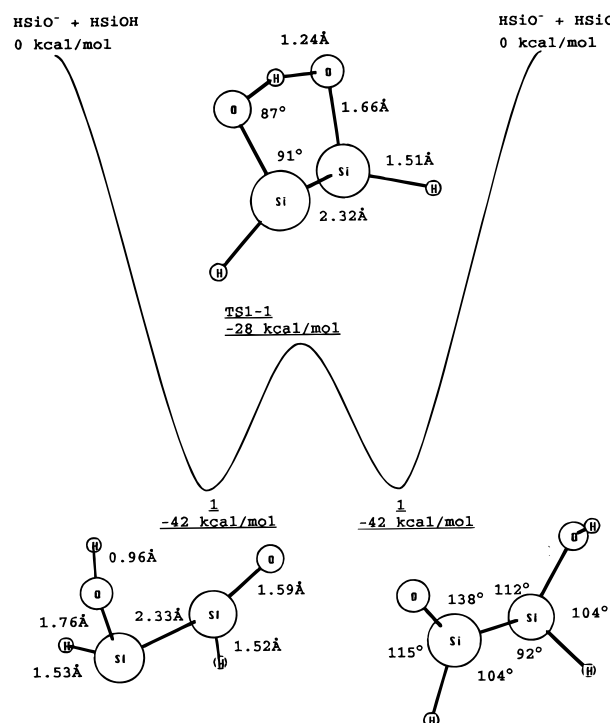


Figure 3. Reaction 1 with MP4 energies, including MP2 zero-point energy corrections. For clarity, the bond angles and distances are respectively indicated on the two mirror images of complex **1**. **TS1-1** has C_2 symmetry.

(including zero-point energy corrections calculated at the MP2/6-31++G(d,p) level of theory) are listed to the right of each reaction.

Several reaction paths and transition states for eqs 1–3 have been located and are displayed in Figures 3–7. Unless otherwise noted, all energies in this discussion are quoted at the MP4/6-311++G(d,p) level of theory, with MP2/6-311++G(d,p) zero-point corrections. The reaction path for identity reaction 1 (Figure 3: $\text{HSiO}^- + \text{HSiOH} \rightarrow \text{HSiOH} + \text{HSiO}^-$) indicates that a stable ion–dipole complex (**1**: –42 kcal/mol) with a silicon–silicon bond forms. Rotation of the OH group about the Si–O bond in the complex results in a symmetric (C_2) proton-transfer transition state (**TS1-1**), which is 14 kcal/mol higher in energy than the ion–dipole complex. Formation of the ion–dipole complex provides more than enough energy for this reaction.

Two pathways for reaction 2 ($\text{HSiO}^- + \text{HSiOH} \rightarrow \text{H}_2\text{SiO} + \text{HSiO}^-$) have been found (Figures 4 and 5). In the first, a four-membered-ring ion–dipole complex (**2**) forms with the two oxygen atoms bridging two silicon atoms (–48 kcal/mol) (Figure 4). A hydrogen on oxygen is trans to the two hydrogen atoms bound to the two silicons. The oxygen-bound hydrogen atom transfers to a bridging position between the oxygen and silicon over a 33 kcal/mol barrier (**TS2-3**). This transition state connects to a second complex (**3**: –83 kcal/mol) that can be thought of as a deprotonated 1,3-cyclodisiloxane. The second proton-transfer path found for reaction 2 involves an initial weak ion–dipole complex (**4**: –16 kcal/mol) surmounting a 4 kcal/mol barrier (**TS4-5**) before falling into a second, deeper well (**5**: –49 kcal/mol) (Figure 5). The weakly bound complex **4** has the OH hydrogen of HSiOH bound to the silicon of HSiO^- .

(30) Schmidt, M. W.; Gordon, M. S. *J. Am. Chem. Soc.* **1991**, *113*, 5244–8.

(31) Pellerite, M. J.; Brauman, J. I. *J. Am. Chem. Soc.* **1983**, *105*, 2672–80.

(32) Craig, S. L.; Brauman, J. I. *Science* **1997**, *276*, 1536–1538.

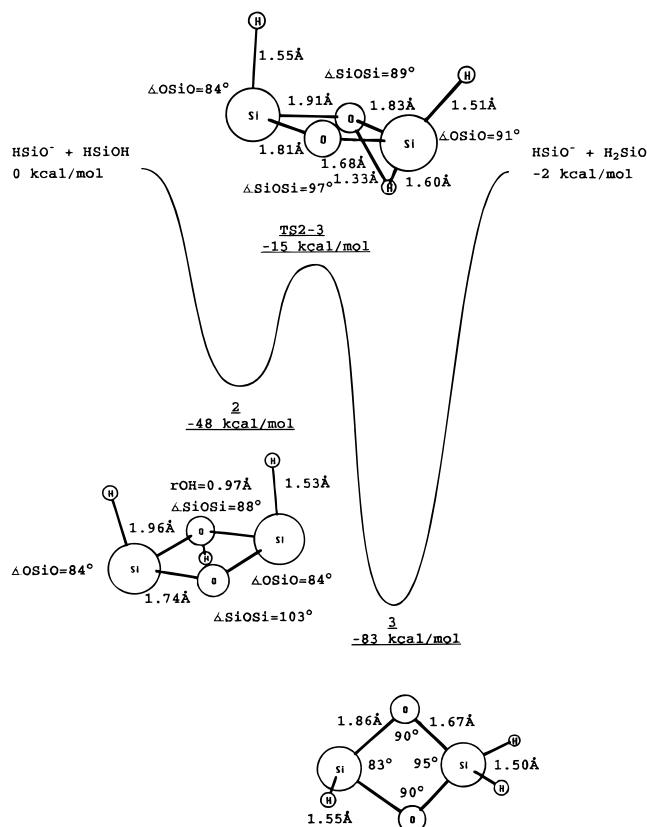


Figure 4. Reaction 2 with MP4 energies and MP2 ZPE corrections. 2 and 3 have C_s symmetry.

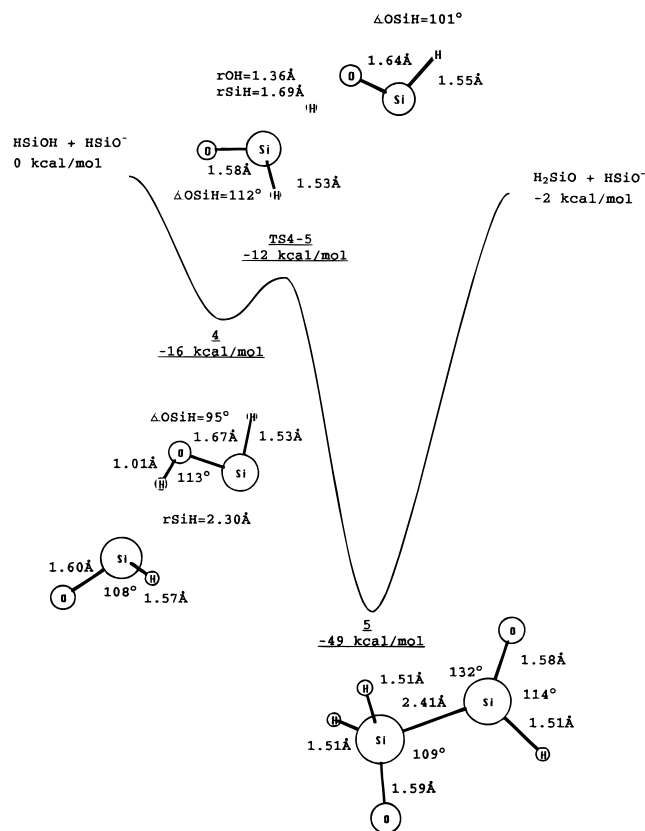


Figure 5. Second route for reaction 2; MP4 energies and MP2 ZPE.

In the transition state, the transferring hydrogen is 1.36 Å from the oxygen and 1.69 Å from the silicon. After that hydrogen

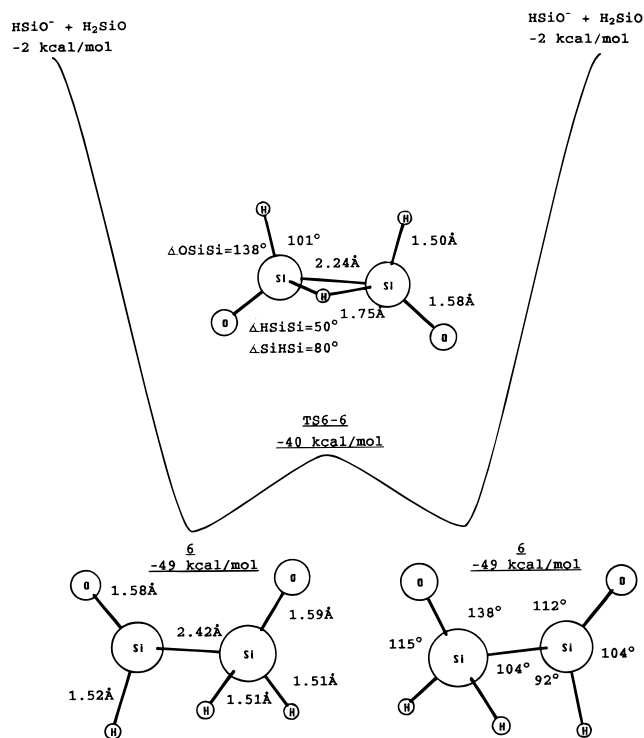


Figure 6. Reaction 3. TS6-6 has C_s symmetry; the two minima are mirror images of complex 6. For clarity, the bond distances are given on the left minimum and the bond angles on the right.

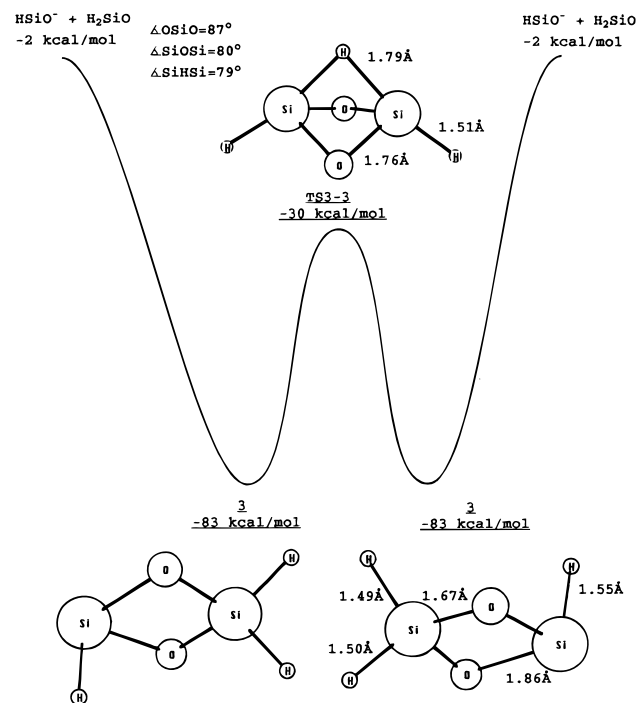


Figure 7. Second path for reaction 3; MP4 energies with MP2 ZPE corrections. TS3-3 has C_{2v} symmetry and 3 is C_s .

is transferred, a strongly bound complex 5 with a silicon–silicon interaction forms.

Two reaction paths for identity reaction 3 ($\text{HSiO}^- + \text{H}_2\text{SiO} \rightarrow \text{H}_2\text{SiO} + \text{HSiO}^-$) are shown in Figures 6 and 7. A silicon–silicon interaction (−49 kcal/mol) in the first of these (Figure 6) leads to a complex 6 that has a small barrier (TS6-6: 9 kcal/mol barrier) to overcome before falling into the second well. The other pathway (Figure 7) involves oxygen atom bridge formation of a complex (3: −83 kcal/mol) and a barrier some

53 kcal/mol higher (**TS3-3**). The intermediate complex (**3**) in this reaction is identical to the deprotonated 1,3-cyclodisiloxane intermediate in Figure 4. Transfer of a hydrogen across the top of the ring as the two ring oxygen atoms move away puckering the ring leads to the transition state (**TS3-3**).

The pathways pictured in Figures 3–7 are interesting to consider further. The two stable structures having silicon–silicon bonds [HOSi(H)SiHO (**1**) and H₂Si(O)SiHO (**5**)] are 45–50 kcal/mol below the energy of the reactants while the two having oxygen bridges (1,3-cyclodisiloxanes) are about 50 and 80 kcal/mol below the entrance channel energy, depending on whether a hydrogen is bonded to a bridging oxygen. The gross features represented here are no more than the consequence of stronger silicon-to-oxygen than silicon-to-silicon bonding. The higher energy of the oxygen-bridged complex with oxygen bearing a hydrogen (Figure 4) is explicable in simple valence bond terms, since the distribution of valence electrons is less favorable in such a structure than in the lower energy complex in which two hydrogen atoms are bound to silicon. The only stable structure that has neither silicon–silicon nor oxygen-bridging interactions is the complex (**4**) with a weak hydrogen-to-silicon bond (Figure 5). The weakness of this interaction is not surprising given the likely atomic charges involved.

The corresponding transition state structures and energies are of three general types as well. The two having silicon–silicon bonds differ only in the way hydrogen is being transferred: one through two oxygen atoms (**TS1-1**) (Figure 3), the other by direct transfer of hydrogen between the silicon atoms (**TS6-6**) (Figure 6). The second type of transition state corresponds to the 1,3-cyclodisiloxane species in which hydrogen is transferred either from oxygen-to-silicon (**TS2-3**) (Figure 4) or across the ring silicon-to-silicon (**TS3-3**) (Figure 7). Finally, the transition state having neither silicon–silicon nor oxygen-bridging interactions (**TS4-5**) (Figure 5) is quite similar to the initially formed weak complex **4** ($r_{\text{OH}} = 1.01 \text{ \AA}$; $r_{\text{SiH}} = 2.30 \text{ \AA}$) with displacement of the hydrogen along the reaction coordinate to a point between oxygen (1.36 Å) and silicon (1.69 Å). The barrier heights in the identity reactions (Figures 3, 6, and 7) are interesting to consider in light of the recent computational work of Gronert²⁹ discussed earlier in which O···H···O transfer had a far lower barrier than Si···H···Si transfer. In the cases studied here, the O···H···O transfer has a 14 kcal/mol barrier (Figure 3), and the two Si···H···Si transfers have 9 and 53 kcal/mol barriers, respectively (Figures 6 and 7). The three transition states considered here are quite different from those discussed by Gronert. They may be thought of as “intramolecular”, rather than intermolecular proton transfers, so a direct comparison is not really possible. We note that a much higher energy requirement is associated with **TS3-3** than **TS6-6**, since **TS3-3** involves a 1,3-transfer while **TS6-6** is a 1,2-transfer.

Despite the interesting features of the structures shown in Figures 3–7, it is clear that these pathways are all accessible for proton transfer. Thus, there is no demonstrably favored pathway that would suggest an unequivocal identification of the parent acid.

(c) Double Proton Transfers. Hydride transfer from an anion to CO₂ is a common gas-phase process, one that HSiO[−] undergoes (HSiO[−] + CO₂ → HCO₂[−] + SiO).² Other HSiO[−] hydride transfers also have been shown to occur with COS, CS₂, and SO₂ (trace only). The related reaction 9



has been studied computationally and is by far the most exothermic of the chemically realistic reactions studied (−24

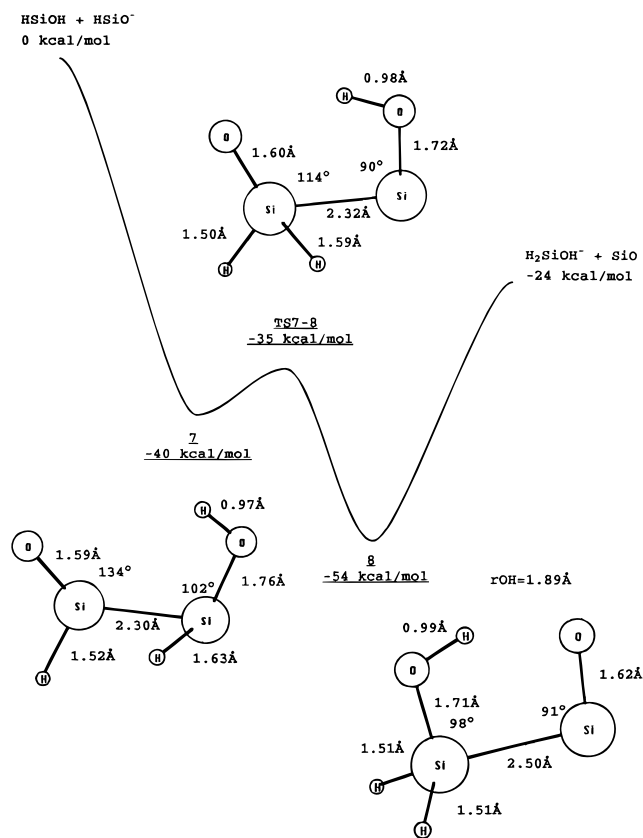


Figure 8. Double proton transfer reaction 9; MP4 energies with MP2 ZPE corrections.

kcal/mol). Although this reaction formally is a hydride transfer, the reaction path shown in Figure 8 is complex and involves two hydrogen transfers, one from silicon-to-silicon followed by one from oxygen-to-oxygen. Thus, the first complex (**7**) forms by silicon–silicon interaction and is 40 kcal/mol below the entrance channel. The hydrogen atom originally bound to silicon in HSiOH is oriented toward the other silicon in this complex. This proton transfers from one silicon to the other as the transition state (**TS7-8**) (5 kcal/mol above complex) is approached. Localized molecular orbital calculations of the transition state indicate a weak hydrogen bond between Si–OH and the oxygen bound to the other silicon. The hydrogen bond is 2.17 Å, while the corresponding O–H bond is 0.98 Å. The second hydrogen transfer leads to a complex (**8**) that is 54 kcal/mol below the reactants. The hydrogen bonding distance in this second complex is 1.89 Å. Although the exothermicity of this reaction suggests that it should be competitive with those discussed in previous paragraphs, there is no evidence that HSiO[−] transfers hydride in this way under FA-SIFT conditions.²

Conclusions

The experimental chemistry of HSiO[−] is rich and complex.² These computational studies have shown that there are several stable, low-energy anion–neutral complexes on the [H₃Si₂O₂][−] potential energy surface, which correspond to species formed by the interaction of HSiO[−] and its conjugate acids, H₂SiO and HSiOH. The key results from this work are the following:

(1) At the highest level of theory used here, the energies of *cis*-HSiOH, *trans*-HSiOH, and H₂SiO are all within a 2 kcal/mol range. Thus, the relative stabilities of these neutral species fall within the likely error bars of these computations. Similarly, the O–H acidities of *cis*-HSiOH and *trans*-HSiOH and the Si–H acidity of H₂SiO fall in a 1 kcal/mol range. As a result,

any of the neutral species could be the source of the most stable anion HSiO^- . These results also suggest that the experimental gas-phase acidity is several kilocalories per mole lower than reported.

(2) The proton transfer reactions illustrated in Figures 3–8 all have in common the characteristic formation of stable ion–molecule complexes ranging from 16 to 83 kcal/mol exothermic relative to separated reactants. These provide a considerable amount of energy with which to drive subsequent reactions. The transition states for the corresponding reactions are well below the reactants and products. Consequently, although all of these reaction paths are energetically accessible, a simple determination of a favored pathway is impossible.

(3) Ion–dipole complex formation is stabilized by distribution of the negative charge throughout complex, primarily centered on the oxygen atoms.

(4) The barriers for “identity” proton transfers are consistent with the earlier work of Gronert ($\text{Si}\cdots\text{H}\cdots\text{Si}$ has a larger barrier

than $\text{O}\cdots\text{H}\cdots\text{O}$), except in the case for which the transfer is facilitated by a direct Si–Si bond.

(5) An unusual “double proton transfer” reaction is quite exothermic and suggests a possible new hydride transfer pathway for HSiO^- .

Acknowledgment. Dedicated to Charles H. DePuy on his 70th birthday. M.S.G. would like to acknowledge support from the Air Force Office of Scientific Research, grant F49 620-95-1-0073. R.D. acknowledges the National Science Foundation (CHE-9223037) for support.

Supporting Information Available: Tables of MP2/6-31++G(d,p), MP4/6-311++G(d,p), and CCSD(T)/6-311++G-(2df,2pd) energies of reactants and combined reactants (1 page, print/PDF). See any current masthead for ordering and Internet access instructions.

JA9722077